Draft version February 5, 2008
Preprint typeset using LaTeX style emulateapj v. 6/22/04

arXiv:astro-ph/0603773v2 5 Sep 2006

JET BREAKS IN SHORT GAMMA-RAY BURSTS. I: THE UNCOLLIMATED AFTERGLOW OF GRB 050724

Dirk Grupe[1], David N. Burrows[1], Sandeep K. Patel[2,3], Chryssa Kouveliotou[3], Bing Zhang[4], Peter Mészáros [1,5],
Ralph A.M. Wijers[6], Neil Gehrels[7]

Draft version February 5, 2008

ABSTRACT

We report the results of the *Chandra* observations of the *Swift*-discovered short Gamma-Ray Burst GRB 050724. *Chandra* observed this burst twice, about two days after the burst and a second time three weeks later. The first *Chandra* pointing occurred at the end of a strong late-time flare. About 150 photons were detected during this 49.3 ks observation in the 0.4-10.0 keV range. The spectral fit is in good agreement with spectral analysis of earlier *Swift* XRT data. In the second *Chandra* pointing the afterglow was clearly detected with 8 background-subtracted photons in 44.6 ks. From the combined *Swift* XRT and *Chandra*-ACIS-S light curve we find significant flaring superposed on an underlying power-law decay slope of α=$0.98^{+0.11}_{-0.09}$. There is no evidence for a break between about 1 ks after the burst and the last *Chandra* pointing about three weeks after the burst. The non-detection of a jet break places a lower limit of 25° on the jet opening angle, indicating that the outflow is less strongly collimated than most previously-reported long GRBs. This implies that the beaming corrected energy of GRB 050724 is at least 4×10^{49} ergs.

Subject headings: GRBs:individual(GRB 050724)

1. INTRODUCTION

Gamma-Ray Bursts (GRBs) are separated into two classes (Kouveliotou et al. 1993; Paciesas et al. 1999): long, soft bursts ($t_{90} >$ 3 s, where t_{90} is the time interval within which 90% of the flux arrives), which are associated with the formation of a black hole during massive star core collapse (Woosley 1993); and short, hard bursts ($t_{90} <$ 3 s), thought to be the result of mergers of compact objects (e.g Eichler et al. 1989; Paczyński 1991; Gehrels et al. 2005; Fox et al. 2005; Barthelmy et al. 2005b; Bloom et al. 2006; Berger et al. 2005). Both types of GRBs are thought to produce a highly relativistic fireball that results in the prompt γ-ray emission through internal shocks in the outflow, and subsequently causes a broad-band afterglow when it shocks the surrounding medium (Mészáros & Rees 1997; Zhang & Mészáros 2004). Much progress has been made since 1997 on the nature of long GRBs, primarily through the study of their radio, optical, and X-ray afterglows, but no afterglows of short GRBs had been detected until 2005, so our understanding of short GRB production mechanisms and environments is still in its infancy. The discoveries by *Swift* and HETE of the afterglows and counterparts for short GRB's 050509B (Gehrels et al. 2005; Bloom et al. 2006), 050709 (Villasenor et al. 2005; Fox et al. 2005; Hjorth et al. 2005), and 050724 (Barthelmy et al. 2005b; Berger et al. 2005) was a tremendous breakthrough in the field, on par with the discovery of the first GRB afterglow by Beppo-SAX (GRB 970228; Costa et al 1997). The X-ray light curve of GRB 050724 displays several flares including a late time flare starting at about 20 ks after the detection of the burst and lasting for about a day (Campana et al. 2006). The early X-ray observations of GRB 050724 by *Swift* also revealed the first *Swift*-discovered dust-scattered halo (Romano et al. 2005a; Vaughan et al. 2005), which was only the second time that an X-ray halo was seen around a GRB afterglow. We report here on combined *Chandra* and *Swift* XRT observations of the X-ray afterglow of GRB 050724, the first high-quality X-ray afterglow of a short burst, and their implications for beaming in this object.

The paper is organized as follows: In §**??** we describe the observations and the data reduction. In §**??** we present the data analysis. The discussion of our results is given in §**??**. Throughout the paper decay and energy spectral indices α and β are defined by $F_\nu(t,\nu) \propto (t-t_0)^{-\alpha}\nu^{-\beta}$, with t_0 the trigger time of the burst. Luminosities are calculated assuming a ΛCDM cosmology with $\Omega_{\rm M}$=0.27, Ω_Λ=0.73 and a Hubble constant of H_0=71 km s^{-1} Mpc^{-1} using the luminosity distances given by Hogg (1999). All errors are 1σ unless stated otherwise.

2. OBSERVATIONS AND DATA REDUCTION

The Burst Alert Telescope (BAT, Barthelmy et al. 2005a) onboard the *Swift* Gamma-Ray-Burst-Explorer Mission (Gehrels et al. 2004) triggered on GRB 050724 at 12:34:09 UT on 2005 July 24 (Covino et al. 2005). The burst had T_{90}=3.0±1.0 s, but most of the flux was released in a hard spike with a duration of 0.25 s (Barthelmy et al. 2005b). Therefore it was considered to be a short GRB. *Swift*'s X-ray Telescope (XRT, Burrows et al. 2005b) began observing the afterglow 74 s after the trigger. GRB 050724 was not detected by

[1] Department of Astronomy and Astrophysics, Pennsylvania State University, 525 Davey Lab, University Park, PA 16802
[2] Universities Space Research Association, 10211 Wincopin Circle, Suite 500 Columbia, MD 21044-3432
[3] NASA/Marshall Space Flight Center, National Space Science Technology Center, VP-62, 320 Sparkman Dr., Huntsville, AL 35805
[4] Department of Physics, University of Nevada, Las Vegas, NV 89154
[5] Department of Physics, Pennsylvania State University, University Park, PA 16802
[6] Astronomical Institute 'Anton Pannekoek', University of Amsterdam, Kruislaan 403, NL-1098 SJ Amsterdam, The Netherlands
[7] NASA Goddard Space Flight Center, Green Belt, MD 20771

Swift's UV-Optical Telescope (UVOT, Roming et al. 2005) and only a 3σ limit of V>18.84 was reported by Chester et al. (2005). Spectroscopic redshifts were reported by Prochaska et al. (2006) (z=0.258±0.002) and Berger et al. (2005) (z=0.257±0.001), who also report on the radio and NIR observations of GRB 050724.

The *Chandra* X-ray Observatory performed two Target of Opportunity observations of GRB 050724. The first occurred two days after the burst at 2005 July 26 20:10 - 2005 July 27 10:45 (UT) for a total of 49.3 ks. The second observation was about three weeks after the burst for a total of 44.6 ks at 2005 August 14 20:29 - 2005 August 15 10:15. All observations were performed in Very-Faint mode with the standard 3.2s read-out time on the on-axis position on the back-illuminated ACIS-S3 CCD. We reprocess all Chandra event data using CIAO $acis_{p}rocess_{e}vents$ and applied VF mode cleaning in order to reduce the ACIS particle background. Source photons were collected in a circular region with $r=1.5''$ and $r=1.0''$ for the first and second *Chandra* observations, respectively. The background photons were selected from the primary event file in a circle with $r=15''$ and $r=10''$, respectively. The data reduction was performed using the *Chandra* analysis software CIAO version 3.3. The X-ray spectrum from the first *Chandra* observation was extracted with the CIAO tool *dmextract* and was analyzed with *XSPEC* version 12.2.1 (Arnaud 1996). The calibration database was CALDB version 3.2.0. The response matrix and the auxiliary response file were created by the CIAO tools *mkrmf* and *mkarf*. The spectrum was rebinned using the FTOOL *grppha* version 3.0.0 to have at least 15 photons per bin.

The *Swift* XRT observed GRB 050724 in the Windowed Timing (WT) and Photon Counting (PC) observing modes (Hill et al. 2004). These X-ray observations have been discussed in detail by Campana et al. (2006) and in this paper we only concentrate on the PC mode data of the later time flare (T>20 ks after the burst) in order to compare the XRT data with our *Chandra* data. The XRT data were reduced by the *xrtpipeline* task version 0.9.9. Source photons were selected by *XSELECT* version 2.3 in a circular region with a radius of $r=47''$ and the background photons in a circular region close by with a radius $r=96''$. For the spectral data only events with grades 0-12 were selected with *XSELECT*. The spectral data were re-binned by using *grppha* having 20 photons per bin. The spectra were analyzed with *XSPEC* version 12.2.1. The auxiliary response files were created by *xrtmkarf* and the standard response matrix swxpc0to12_20010101v008.rmf was used.

Background-subtracted X-ray flux light curves in the 0.3-10.0 keV energy range of the *Chandra* and *Swift* observations were constructed using the ESO Munich Image Data Analysis Software *MIDAS* (version 04Sep). The count rates were converted into unabsorbed flux units using energy conversion factors (ECF) which were determined by calculating the count rates and the unabsorbed fluxes in the 0.3-10.0 keV energy band using XSPEC as described in Nousek et al. (2006). The ECFs are 8.3×10^{-11} ergs s^{-1} cm^{-2} counts^{-1} for the *Swift* observation 1.6×10^{-11} ergs s^{-1} cm^{-2} counts^{-1} for the *Chandra* observations.

3. DATA ANALYSIS

3.1. *Position*

The first *Chandra* observation found a single source located within the *Swift* XRT error circle at RA (J2000) = $16^{\rm h}24^{\rm m}44.^{\rm s}36$, Dec (J2000) = $-27^\circ32'27.''5$, with an error radius of $0.''5$ (Burrows et al. 2005d). This places the X-ray afterglow $1.''0$ south of the center of an elliptical galaxy (Barthelmy et al. 2005b; Berger et al. 2005), coincident with the optical afterglow position reported by Berger et al. (2005) and with the VLA radio position given by Berger et al. (2005) and Soderberg (2005).

3.2. *Light curve*

The left panel of Figure 1 displays the 0.3-10 keV unabsorbed flux light curve of the *Swift* XRT PC mode and *Chandra* ACIS-S observations. Table 1 lists the times and fluxes of the *Swift* and *Chandra* observations. Following the early very steep decay (between 100 and 300 s; see Campana et al. (2006)), the light curve is well fit by a single underlying power law decay slope of $\alpha=0.98^{+0.11}_{-0.09}$ (indicated by the dotted line in Figure 1), with one small and one very large flare superposed. The slope was determined from a linear regression fit to the four underlying afterglow data points in the *Swift* XRT light curve plus the final *Swift* XRT data point. Note, that the last XRT data point is just a marginal detection at the 2σ level containing a total observing time of 47.1 ks. The afterglow decay slope $\alpha=0.98$ deviates from the slope $\alpha=0.60\pm0.20$ given in Campana et al. (2006). We analyzed our afterglow light curves by using different fitting routines within XSPEC, IDL, and MIDAS and always found a decay slope $\alpha \approx 1.0$. Most likely the difference between our decay slope and that found by Campana et al. (2006) is due to different binning methods and/or treatment of the various flares that complicate modeling the underlying afterglow.

The largest flare occurs about 50ks after the burst. This flare has a fluence of 7.7×10^{-8} ergs cm^{-2} (Campana et al. 2006). The first *Chandra* observation from 2005-July-26/27 occurred at the end of this late-time flare. While the afterglow was almost undetectable with the *Swift* XRT, *Chandra* was able to detect 150 source photons in the 49.3 ks observation in the 0.4-10.0 keV band. A combined XRT and ACIS-S light curve of the decaying flare as displayed in the right panel of Figure 1 results in a decay slope $\alpha=2.98^{+01.6}_{-0.13}$ ($\chi^2/\nu = 9.8/14$).

During the second *Chandra* observation three weeks after the burst 8 background-subtracted source photons were detected in 44.6 ks. As shown in the left panel of Figure 1 this last data point is consistent with a flat decay slope $\alpha=0.98$, representing the underlying afterglow due to the forward external shock in the ambient medium. There is no sign of a jet break in the light curve up to the final *Chandra* point three weeks after the burst.

3.3. *Spectral Analysis*

Figure 2 displays the *Chandra* ACIS-S spectrum of GRB 050724. This spectrum was obtained during the decay of the late-time flare in the light curve of GRB 050724 (left panel of Figure 1). This spectrum can be well-fitted by a single absorbed power law (using $wabs * powl$ in *XSPEC*). The results of the fits to the X-ray data are listed in Table 2. A free fit to the data results in an absorption column density at z=0 of $N_{\rm H}$=$5.86^{+6.32}_{-2.99} \times 10^{21}$ cm^{-2}, which is significantly in excess of the Galactic value $N_{\rm H}$=1.48×10^{21} cm^{-2} given by Dickey & Lockman (1990). However, as noticed by Vaughan et al. (2005), the line-of-sight of GRB 050724 passes close to the Ophiuchus molecular cloud and the Galactic column density is therefore significantly higher than what is given by Dickey & Lockman (1990). Vaughan et al. (2005) estimated the real value of the Galactic column density to be 3.4-4.2$\times10^{21}$ cm^{-2}. Therefore the fit to the *Chandra* ACIS-S data is consistent with the Galactic value and no additional absorption is required. Figure 2 displays the single power law fit to the *Chandra* ACIS-S data. The left panel of Figure 2 shows the ACIS-S spectrum and the right panel displays a contour plot of the absorption column density $N_{\rm H}$ and the photon spectral index Γ=$\beta_{\rm X}$+1. We conclude that no intrinsic absorber is required in the host galaxy. The X-ray energy spectral slope as listed in Table 2 is $\beta_{\rm X}$=$0.86^{+0.34}_{-0.31}$, where the absorption column density is fixed to the Galactic value with $N_{\rm H}$=4.0×10^{21}cm^{-2} as given by Vaughan et al. (2005).

For comparison, we examine the *Swift* XRT spectrum of the late-time flare of GRB 050724, shown in Figure 3. As listed in Table 2, our analysis of the XRT data of the late time flare (T>20 ks after the burst) results in an energy spectral index $\beta_{\rm X}$=$0.85^{+0.28}_{-0.36}$ when the absorption column density is left as a free parameter. The absorption column density $N_{\rm H}$=$4.44^{+2.13}_{-2.52} \times 10^{21}$cm^{-2} also agrees with the Galactic absorption column density as given by Vaughan et al. (2005) and does not require any additional absorption. This result agrees well with the analysis reported by Campana et al. (2006). The right panel of Figure 3 displays the contour plot between the absorption column density $N_{\rm H}$ and the photon index Γ.

Table 2 also lists the results from a joint fit to the *Chandra* ACIS-S and *Swift* XRT spectra. This joint fit yields similar results to those obtained from the separate spectral fits.

The *Chandra* spectral analysis from the fading tail of this flare is in excellent agreement with the spectral fit for the flare as a whole, confirming the conclusion of Campana et al. (2006) that there is no evidence for spectral evolution in this afterglow.

4. DISCUSSION

The main result of our late time *Chandra* observation is that there is no jet break observed in the X-ray afterglow of GRB 050724. Our last Chandra data point connects to the lower envelope of the XRT data points before $\sim$ 20 ks as a single power law decay with α=$0.98^{+0.11}_{-0.09}$. We interpret this slope as the afterglow from the forward shock, extending from $\sim$ 0.5 ks after the burst until after the last *Chandra* observation 3 weeks later, with flaring superposed on this steady decay. Following the slow cooling ISM case listed in Table 1 in Zhang & Mészáros (2004) we find that the slope of the electron spectrum is $p = 2.70$ and that the observed emission frequency ν is $\nu_{\rm m} < \nu < \nu_{\rm c}$ with $\nu_{\rm m}$ the injection frequency and $\nu_{\rm c}$ the cooling frequency (See Zhang & Mészáros 2004, for details.).

The non-detection of a jet break up until 22 days after the burst places constraints on the jet opening angle. Using the relations given by Sari et al. (1999) and Frail et al. (2001), we can estimate the jet opening angle as:

$$\Theta > 25^\circ \left(\frac{n}{0.1}\right)^{1/8} \left(\frac{E_{\gamma,\rm iso}}{4\times10^{50}}\right)^{-1/8} \qquad (1)$$

using an ambient medium density of $n = 0.1$ cm^{-3}, an isotropic equivalent energy of 4 $\times10^{50}$ ergs s^{-1} and an isotropic-equivalent kinetic energy of $E_{\rm k,iso} = 1.5\times10^{51}$ ergs, and an efficiency of the fireball $\eta = \frac{E_{\rm K,iso}}{E_{\gamma,\rm iso}}$=0.2, as given by Berger et al. (2005). If the density is as high as 10^3 cm^{-3} (Panaitescu 2006), the inferred jet angle must be larger than 79°.

This result differs from the conclusions of Panaitescu (2006) and Berger et al. (2005), who estimated an opening angle of $8^\circ - 12^\circ$ based on the radio and NIR observations of the afterglow of GRB 050724. The radio data seem to suggest an early jet break about 1–2 days after the burst, based on the steep radio decay slope $\alpha_{\rm radio}$=2.0, but the paucity of both the optical and radio observations and the possibility of strong Galactic interstellar scintillation in the 8.5 GHz radio band make this conclusion uncertain (Panaitescu 2006). In addition, we point out that both the optical and radio data occur on the declining side of the large X-ray flare. If this flare is caused by central engine activity, the optical and radio behavior may be related to this flare rather than to a jet break. In any case, since a jet break is expected to be achromatic, the *Chandra* data strongly rule out a jet break at one day post-burst. The energy of the prompt emission is 3×10^{50} ergs (Barthelmy et al. 2005b) while the energy in the late-time flare is 2×10^{49} ergs (Campana et al. 2006) which is about 7% of the energy of the prompt emission. This result supports central engine models which predict a reduced activity at later times (e.g. Zhang & Mészáros 2004).

Until recently, no jet break has ever been convincingly found in a short GRB afterglow. Fox et al. (2005) discussed the possibility of a jet break in the HETE-2-discovered short burst GRB 050709. However, their conclusions are based on few data points that poorly constrain jet parameters (Panaitescu 2006) and may be open to other interpretations, particularly given the complex nature of X-ray afterglows, even for short GRBs (e.g. GRB 050724). The only convincing case of a jet break found in a short GRB afterglow is GRB 051221A (Burrows et al. 2006, Paper II), based on detailed, well-sampled *Swift* and *Chandra* observations.

The large lower limit of the jet angle inferred from our data suggests that the jet of this particular short GRB is much less collimated than typical long GRBs reported in previous works (Frail et al. 2001; Bloom et al. 2003; Soderberg et al. 2006), although we note that *Swift* afterglows in general may not support those early results (Sato et al. 2006, in preparation; Willingale et al. 2006, in preparation). The elliptical host galaxy of GRB 050724 suggests that the progenitor is not a collapsar and is likely a compact star merger (NS-NS or NS-BH). The wide jet angle inferred from the data is consistent with such a progenitor scenario (e.g. Mészáros, Rees, & Wijers 1999), since there is no extended massive stellar envelope as in long GRBs that serves to naturally collimate the outflow (e.g.

Zhang, Woosley, & Heger 2004). Numerical simulations of mergers (e.g. Aloy et al. 2005) suggest a varying degree of short GRB collimation angles, which are in general wider than those of long GRBs. A wide angle also potentially explains why short GRBs are less bright (e.g. Mészáros, Rees, & Wijers 1999). The total energy budget (collimation corrected) of short GRBs then should not be orders of magnitudes lower than that of long GRBs. Swift observations show that short GRBs typically have a very low isotropic gamma-ray energy given their very low redshifts (e.g. Gehrels et al. 2005; Barthelmy et al. 2005b; Fox et al. 2005). However, if short GRBs typically have wide jets, this would reduce the large gap in the total energy budget of short and long GRBs implied by the isotropic energies, which differ by several orders of magnitude (Frail et al. 2001) under the assumption of similar jet angles. Applying the beaming correction of $(1 - cos\Theta)$ as given by Sari et al. (1999) and Rhoads (1999) and using the isotropic energy given by Berger et al. (2005) of $E_{\gamma,\rm iso} = 4 \times 10^{50}$ ergs, the beaming corrected energy of GRB 050724 is 4×10^{49} to 4×10^{50} ergs, depending on the beaming angle. This energy is comparable with the modest fireball energies predicted from neutron star - neutron star mergers based on neutrino - anti-neutrino annihilation as given by, e.g., Popham et al. (1999).

The long measurement baseline for the afterglow slope enabled by the late *Chandra* observation also guides the interpretation of the late flare, making it clear that the rapid decline in the X-ray light curve after 60 ks is the decay of a flare and not a jet break. In the *Swift* era, X-ray flares have generally been interpreted as due to late central engine activity (Burrows et al. 2005c; Zhang et al. 2006; Falcone et al. 2006; Romano et al. 2006). Zhang et al. (2006) pointed out that the steep decay ($\alpha \sim 2.70$) after this flare may be an indication of the curvature effect of a late internal dissipation activity. Liang et al. (2006) have tested such a model by searching for the required time zero point of this flare to satisfy the curvature effect interpretation and found that it is right at the rising part of the flare. Our late Chandra data point suggests that this flare is an independent component that is superimposed on the otherwise power-law decaying afterglow component. This flare may then originate from a different emission site, adding credence to the late central engine activity interpretation.

This is a particularly long and bright flare for such late times, and it is surprising to find it in a short GRB afterglow, since models of NS-NS mergers have typically suggested rapid creation of a black hole with little material left over to feed the central engine at such late times. These observations suggest that the central engine of GRB 050724 may have reactivated at around a day after the burst, which calls for central engine models that can extend the short GRB central engine to such a late time. Possible scenarios include fragmentation of a neutron star by a black hole in a NS-BH merger (Faber et al. 2006), fragmentation of the accretion disk (Perna et al. 2006), a magnetic-barrier-modulated accretion flow (Proga & Zhang 2006), or the magnetic activity of a post-merger massive neutron star (Dai et al. 2006). Future extensive afterglow observations and more detailed theoretical modeling will be required to further understand the progenitor and the central engine of short GRBs.

Our observations of GRB 050724 have demonstrated the importance of late time *Chandra* observations of GRB afterglows. Our last *Chandra* observation from 2005 August provides crucial information about the late time behavior of the afterglow that no other X-ray observatory is able to measure at these low flux levels. Further late time X-ray observations of GRB afterglows will provide an improved understanding of the characteristics of jets of both long and short GRBs.

We would like to thank the anonymous referee for varous comments and suggestions to improve the paper, and Sergio Campana for discussions on the XRT light curve. This research has made use of data obtained through the High Energy Astrophysics Science Archive Research Center Online Service, provided by the NASA/Goddard Space Flight Center. This research was supported by NASA contract NAS5-00136 and SAO grant G05-6076X BASIC.

REFERENCES

Aloy, M.A., Janka, H.-T., Müller, E., 2005, A&A, 436, 273
Arnaud, K. A., 1996, ASP Conf. Ser. 101: Astronomical Data Analysis Software and Systems V, 101, 17
Barthelmy, S.D., et al. 2005a, Space Science Reviews, 120, 143
Barthelmy, S.D., et al. 2005b, Nature, 438, 994
Berger, E., et al., 2005, Nature, 438, 988
Bloom, J.S., Frail, D.A., & Kulkarni, S.R., 2003, ApJ, 594, 674
Bloom, J.S., et al., 2006, ApJ, 638, 354
Burrows, D.N., Hill, J.E., Chincarini, G., et al., 2005a, ApJ, 622, L85
Burrows, D.N., et al., 2005b, Space Science Reviews, 120, 165
Burrows, D. N. et al. 2005c, Science, 309, 1833
Burrows, D.N., Grupe, D., Kouveliotou, C., Patel, S., Meszaros, P., Zhang, B., and Wijers, R.A.M.J., 2005d, GCN 3697
Burrows, D.N., et al. 2006, ApJ, accepted, astro-ph/0604320
Campana, S., et al., 2006, A&A, 454, 113
Chester, M., et al., 2005, GCN 3670
Costa, E., et al., 1997, Nature, 387, 783
Covino, S., et al., 2005, GCN 3665
Dai, Z. G., Wang, X. Y., Wu, X. F. & Zhang, B. 2006, Science, 311, 1127
Dickey, J.M., & Lockman, F.J., 1990, ARA&A, 28, 215
Eichler, D., Livio, M., Piran, T., & Schramm, D.N., 1989, Nature, 340, 126
Faber, J. A., Baumgarte, T. W., Shapiro, S. L., and Taniguchi, K. 2006, ApJ, submitted, astro-ph/0603277
Falcone, A. et al. 2006, ApJ, 641, 1010
Fox, D.B., et al., 2005, Nature, 437, 845
Frail, D.A., Kulkarni, S.R., Sari, R., et al., 2001, ApJ, 562, L55
Gehrels, N., et al., 2004, ApJ, 611, 1005
Gehrels, N., et al., 2005, Nature, 437, 851
Hill, J.E., et al., 2004, SPIE, 5165, 217
Hjorth, J., et al., 2005, Nature, 437, 859
Hogg, D., 1999, astro-ph/9905116
Kouveliotou, C., et al., 1993, ApJ, 541, L101
Liang, E. et al. 2006, ApJ, accepted, astro-ph/0602142
Mészáros , P., & Rees, M. J. 1997, ApJ, 476, 232
Mészáros, P., Rees, M. J., Wijers, R. 1999, New Astron. 4, 303
Nousek, J., Kouveliotou, C., Grupe, D., Page, K.L., et al., 2006, ApJ, 642, 389
Paciesas, W.S., et al., 1999, ApJS, 122, 465
Paczyński, B., 1991, Acta Astron., 41, 257
Panaitescu, A., 2006, MNRAS, 367, 42
Perna, R., Armitage, P.J., & Zhang, B., 2006, ApJ, 636, L29
Popham, R., Woosley, S.E., & Freyer, C., 1999, ApJ, 518, 356

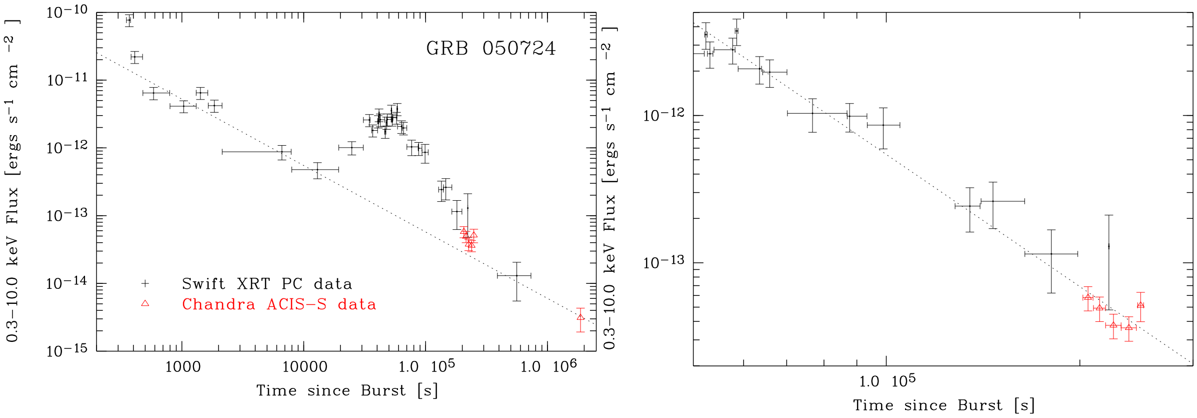

Fig. 1.— *Swift* XRT PC mode and *Chandra* ACIS-S light curve of the afterglow of GRB 050724. The light curve shows the observed 0.3-1.0 keV unabsorbed flux. The right panel displays the *Swift* XRT and *Chandra* ACIS-S light curves of the decline of the late time flare. The dotted lines display the decay slopes of the afterglow (left, α=0.98$^{+0.11}_{-0.09}$), and the flare decay (right, $\alpha = 2.98^{+0.16}_{-0.13}$).

Prochaska, J.X., et al., 2006, ApJ, 642, 1160
Proga, D., & Zhang, B., 2006, MNRAS, 370, 61
Rhoads, J.E., 1999, ApJ, 487, 737
Romano, P., et al., 2005, GCN 3685.
Romano, P. et al. 2006, A&A, 450, 59
Roming, P.W.A., et al., 2005, Space Science Reviews, 120, 95
Sari, R., Piran, T., & Halpern, J.P., 1999, ApJ, 519, L17
Soderberg, A.M., 2005, GCN 3696
Soderberg, A. M., et al., 2006, ApJ, in press, astro-ph/0601455
Vaughan, S., et al., 2005, ApJ, 639, 323
Villasenor, J.S., et al., 2005, Nature, 437, 855
Woosley, S.E., 1993, ApJ, 405, 273
Zhang, B., & Mészáros , P., 2004, Int. Journal of Modern Physics A, Vol. 19, No. 15, 2385
Zhang, B., Fan, Y.Z., Dyks, J., Kobayashi, S., Mészáros , P., Burrows, B.N., Nousek, J.A., & Gehrels, N., 2006, ApJ, 642, 354
Zhang, B., 2005b, Proc. of "Astrophysics Sources of High Energy Particles and Radiation" (eds. T. Bulik, G. Madejski and B. Rudak), AIP conf. proc., Vol 801, 106
Zhang, W., Woosley, S. E. & Heger, A. 2004, ApJ, 608, 365

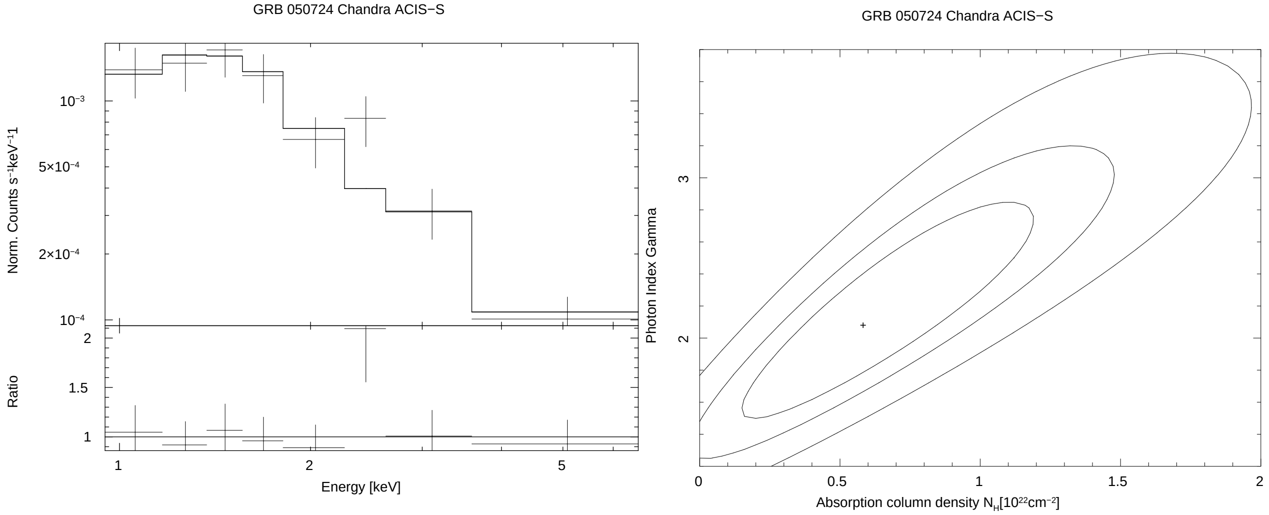

FIG. 2.— *Chandra* ACIS-S3 spectrum. The left panel displays the X-ray spectrum with an absorbed power law model fitted to the data. The right panel shows the contour plot between the absorber column density and the photon index $\Gamma = \beta_X + 1$. The Galactic column density as given by Vaughan et al. (2005) is $N_H = 3.4 - 4.2 \times 10^{21}$ cm^{-2}. The contour levels are 1, 2, and 3 σ.

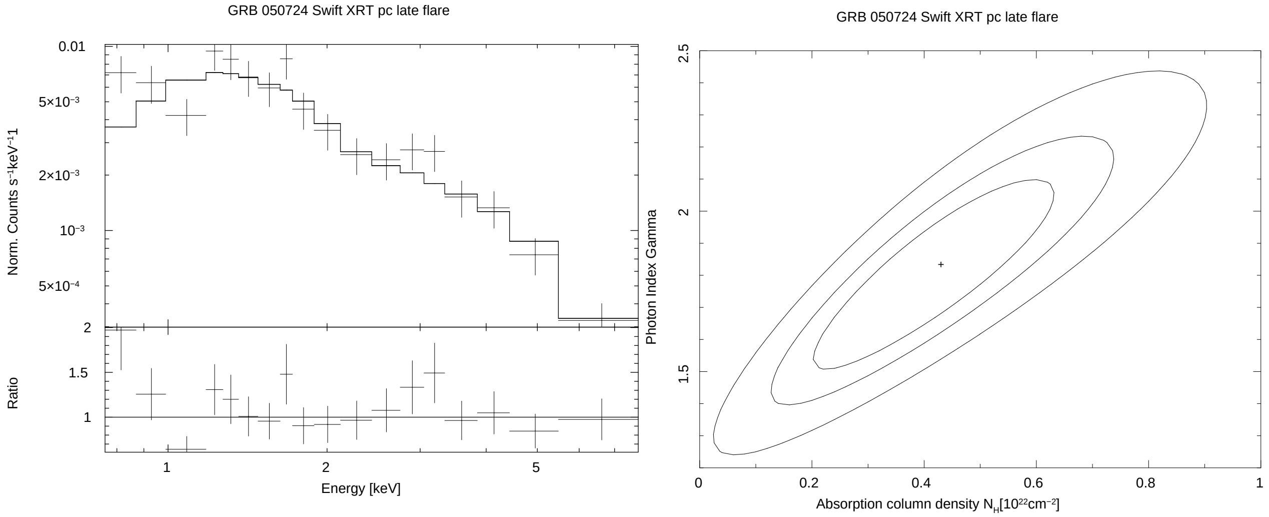

FIG. 3.— *Swift* XRT PC mode spectrum. The left panel displays the X-ray spectrum with an absorbed power law model fitted to the data. The right panel shows the contour plot between the absorber column density and the photon index $\Gamma = \beta_X + 1$. The Galactic column density as given by Vaughan et al. (2005) is $N_H = 3.4 - 4.2 \times 10^{21}$ cm^{-2}. The contour levels are 1, 2, and 3 σ.

TABLE 1

Swift XRT and *Chandra* light curve data of GRB 050724

Observatory	Time after burst[1]	$T_{\rm obs}$[1]	Flux[2]	Flux error[2]
Swift	348	15	1.40×10^{-10}	0.28×10^{-10}
	370	28	7.68×10^{-11}	1.53×10^{-11}
	410	95	2.20×10^{-11}	0.45×10^{-11}
	586	318	6.45×10^{-12}	1.33×10^{-12}
	1035	514	4.12×10^{-12}	0.82×10^{-12}
	1421	323	6.48×10^{-12}	1.31×10^{-12}
	1847	493	4.20×10^{-12}	0.86×10^{-12}
	6625	2033	8.75×10^{-13}	2.12×10^{-13}
	12960	3415	4.77×10^{-13}	1.27×10^{-13}
	24813	1910	1.00×10^{-12}	0.22×10^{-12}
	34556	805	2.58×10^{-12}	0.53×10^{-12}
	36840	1158	1.81×10^{-12}	0.37×10^{-12}
	40898	830	2.47×10^{-12}	0.51×10^{-12}
	41485	652	3.08×10^{-12}	0.65×10^{-12}
	42476	772	2.60×10^{-12}	0.55×10^{-12}
	46608	1196	1.73×10^{-12}	0.36×10^{-12}
	47881	880	2.35×10^{-12}	0.48×10^{-12}
	48481	790	2.62×10^{-12}	0.54×10^{-12}
	52419	587	3.53×10^{-12}	0.72×10^{-12}
	53191	800	2.62×10^{-12}	0.53×10^{-12}
	57706	759	2.79×10^{-12}	0.56×10^{-12}
	58551	554	3.74×10^{-12}	0.77×10^{-12}
	63527	972	2.07×10^{-12}	0.44×10^{-12}
	65890	1023	1.96×10^{-12}	0.42×10^{-12}
	76802	1639	1.03×10^{-12}	0.26×10^{-12}
	87692	1973	9.88×10^{-13}	2.16×10^{-13}
	98926	1208	8.59×10^{-13}	2.66×10^{-13}
	134892	4438	2.43×10^{-13}	0.81×10^{-13}
	146538	3952	2.62×10^{-13}	0.91×10^{-13}
	180599	6980	1.15×10^{-13}	0.53×10^{-13}
	221928	2121	1.29×10^{-13}	0.81×10^{-13}
	560000	47109	1.30×10^{-14}	0.75×10^{-14}
Chandra	205920	8270	5.80×10^{-14}	1.08×10^{-14}
	214612	9610	4.93×10^{-14}	0.93×10^{-14}
	225551	12546	3.76×10^{-14}	0.72×10^{-14}
	238353	13065	3.62×10^{-14}	0.69×10^{-14}
	248605	6465	5.14×10^{-14}	1.16×10^{-14}
	1867280	43218	3.12×10^{-15}	1.20×10^{-15}

[1] In units of s.

[2] In units of ergs s^{-1} cm^{-2}.

TABLE 2

Power law fits to the X-ray spectrum of GRB 050724

Observation	$N_{\rm H}$[1]	$\beta_{\rm X}$	χ^2/ν
Chandra ACIS-S	$5.86^{+6.32}_{-2.98}$	$1.08^{+0.82}_{-0.42}$	4.6/5
	4.00 (fix)	$0.86^{+0.34}_{-0.31}$	5.3/6
Swift XRT	$4.44^{+2.13}_{-2.52}$	$0.85^{+0.28}_{-0.36}$	20/15
	4.00 (fix)	$0.79^{+0.16}_{-0.15}$	20/16
ACIS-S + XRT	$4.41^{+2.49}_{-1.49}$	$0.85^{+0.29}_{-0.14}$	26/21
	4.00 (fix)	$0.81^{+0.15}_{-0.14}$	26/22

[1] Galactic absorption column density in units of 10^{21} cm^{-2}. For the Galactic value we use 4.0×10^{21} cm^{-2} as given by Vaughan et al. (2005)